ARMY RESEARCH LABORATORY

Considerations for the Design of a Multi-Color High-Speed X-Ray Computed Tomography Diagnostic

by Michael B. Zellner, Gerard T. Chaney, Chester A. Benjamin, Ronald Cantrell, Robert W. Borys, Robin D. Strickland, Joshua M. Sturgill, James A. Perrella, Gerald L. Schafer, Corey E. Yonce, Martin L. Potter, Stephen Alleyne, and John M. Zajicek

ARL-TR-6969 **June 2014**

NOTICES

Disclaimers

The findings in this report are not to be construed as an official Department of the Army position unless so designated by other authorized documents.

Citation of manufacturer's or trade names does not constitute an official endorsement or approval of the use thereof.

Destroy this report when it is no longer needed. Do not return it to the originator.

Army Research Laboratory
Aberdeen Proving Ground, MD 21005-5066

ARL-TR-6969 **June 2014**

Considerations for the Design of a Multi-Color High-Speed X-Ray Computed Tomography Diagnostic

Michael B. Zellner, Gerard T. Chaney, Chester A. Benjamin, Robin D. Strickland, Martin L. Potter, and John M. Zajicek
Weapons and Materials Research Directorate, ARL

Ronald Cantrell, Robert W. Borys, Gerald L. Schafer, Corey E. Yonce, and Stephen Alleyne
Bowhead Science & Technology

Joshua M. Sturgill and James A. Perrella
Dynamic Science Inc.

REPORT DOCUMENTATION PAGE	Form Approved OMB No. 0704-0188

1. REPORT DATE *(DD-MM-YYYY)*	2. REPORT TYPE	3. DATES COVERED (From - To)
June 2014	Final	October 2013–September 2014

4. TITLE AND SUBTITLE
Considerations for the Design of a Multi-Color High-Speed X-Ray Computed Tomography Diagnostic

5a. CONTRACT NUMBER

5b. GRANT NUMBER

5c. PROGRAM ELEMENT NUMBER

6. AUTHOR(S)
Michael B. Zellner, Gerard T. Chaney, Ronald Cantrell, Robert W. Borys, Chester A. Benjamin, Robin D. Strickland, Joshua M. Sturgill, James A. Perrella, Gerald L. Schafer, Corey E. Yonce, Martin L. Potter, Stephen Alleyne, and John M. Zajicek

5d. PROJECT NUMBER
AH80

5e. TASK NUMBER

5f. WORK UNIT NUMBER

7. PERFORMING ORGANIZATION NAME(S) AND ADDRESS(ES)
U.S. Army Research Laboratory
ATTN: RDRL-WMP-D
Aberdeen Proving Ground, MD 21005-5066

8. PERFORMING ORGANIZATION REPORT NUMBER
ARL-TR-6969

9. SPONSORING/MONITORING AGENCY NAME(S) AND ADDRESS(ES)

10. SPONSOR/MONITOR'S ACRONYM(S)

11. SPONSOR/MONITOR'S REPORT NUMBER(S)

12. DISTRIBUTION/AVAILABILITY STATEMENT
Approved for public release; distribution is unlimited.

13. SUPPLEMENTARY NOTES

14. ABSTRACT
This report describes the development and work progress of designing and building an improved radiographic computed tomographic technique that has the potential to provide material specificity of a three-dimensional spatial field, relatively quickly in time (on the order of <100 ns), with mm^3 voxel resolution (a voxel is the three-dimensional equivalent of a pixel). This report details thoughts and work performed focusing on potential issues regarding: the robustness of a structural frame and components of the diagnostic; how to obtain accurate measurements of the x-ray flux verses energy output of the multiple x-ray sources, which is necessary to obtain material specificity; electrical grounding and shielding of the numerous pulse power sources; and collection of static data that can be used to prove the premise of material specificity in a nondynamic state. Conclusions are made suggesting possible paths forward for construction of a device that would have the potential to make measurements of dynamic events with high-impulse loadings.

15. SUBJECT TERMS
computed tomography, x-ray, energy-selective, three-dimensional

16. SECURITY CLASSIFICATION OF:			17. LIMITATION OF ABSTRACT	18. NUMBER OF PAGES	19a. NAME OF RESPONSIBLE PERSON
a. REPORT	b. ABSTRACT	c. THIS PAGE			Michael B. Zellner
Unclassified	Unclassified	Unclassified	UU	26	19b. TELEPHONE NUMBER (*Include area code*) 410-306-2565

Standard Form 298 (Rev. 8/98)
Prescribed by ANSI Std. Z39.18

Contents

List of Figures

List of Tables

INTENTIONALLY LEFT BLANK.

1. Introduction

The task of understanding how a material responds under a dynamic environment is very difficult. It is ultimately difficult because there are many subatomic entities that all respond in a chain-reaction process to the initial, and possibly continuing, forces applied to a system. In an attempt to partially understand material response for predictive applications, scientists observe material interactions at some level and hypothesize theories that describe phenomena such as fracture, chemical reactions, and electrical conduction. However, these theories are often incomplete, limited by the spatial and temporal resolution with which the scientist can make the observations.

This report describes the development of an improved radiographic computed tomographic technique that has the potential to provide material specificity of a three-dimensional spatial field, relatively quickly in time (on the order of <100 ns), with mm^3 voxel resolution (a voxel is the three-dimensional equivalent of a pixel). This diagnostic is an extension of work in which Moser et al. (*1*) used flash x-radiograph sources to acquire numerous two-dimensional radiographs that were subsequently used to reconstruct a three-dimensional radiograph. It was then combined with work demonstrating that discrete energy sources can be applied to conventional (long timescale) x-ray computed tomography to discern material specificity (*2*). Because of the short acquisition timescales, the potential to resolve multiple materials, and the ability to resolve the materials in three spatial dimensions, this diagnostic may demonstrate usefulness in any field that involves dynamic material response phenomena such as material mixing, material flow, material fracture, material densification, etc.

The theory governing functionality of multi-color (multi-energy) high-speed computed tomography was conceived during deliberations at the Tomodamage 2012 conference in Freiburg, Germany. Moser et al. (*1*) presented a technique that constructed a three-dimensional x-ray radiograph of a steel bullet penetrating a ceramic disk from two-dimensional radiographs of a target acquired from different angles, simultaneously. The diagnostic used six 450-KeV sources and six imaging plate x-ray detectors to record six two-dimensional images. The three-dimensional reconstruction of an x-ray attenuation (or transmission) image was enabled through implementation of an improved multiplicative algebraic reconstruction technique (*3*, *4*). This iterative algorithm is optimized for reconstruction of a field variable, such as x-ray attenuation, when sparsely populated and incomplete projections are acquired in trade for long-computational time. Because there are multiple materials in Moser's (*1*) experiment and the materials undergo a compression to an unknown density state, it becomes impossible to differentiate between materials; therefore, one is not able to discern where the ceramic is relative to the steel of the bullet. At this time it was recognized that, because the geometry of the materials are known in three spatial dimensions, the Beer-Lambert law could be applied and N x-ray energies could be

used to discern N materials assuming that the standard x-ray attenuation absorption coefficients (*5*) are not strongly influenced by material compression (densification):

$$I(E) = I_0 e^{-\frac{\mu(E)}{\rho}\rho x} \tag{1}$$

where *I(E)* is the intensity as a function of energy (*E*) in power/area^2, I_0 = initial beam intensity in power/area^2, $\mu(E)/\rho$ is the mass attenuation coefficient in cm^2/g as a function of energy, ρ is the material density in g/cm^3, and x is the through thickness length in centimeters. It was later found that application of multiple discrete energy x-ray sources to conventional computed tomography had already proved functionality at defining material specificity (*2*). However, when attempting to apply computed tomography to fast dynamic events, such as that which would occur in the timeframe of a ballistic event or as a fast moving object passing through the diagnostics field of view, it is necessary to increase the flux of photons contributing to the scattering event so that sufficient contrast can be attained in the radiographs. For these types of experiments a high-flux source such as flash discharge x-ray sources is necessary. This complicates the material specificity analysis proved previously (*2*) in that now *I(E)* of equation 1 is implemented as a function instead of a discrete value.

This report continues to discuss some specific aspects of the construction of a multi-color system including: design of a robust frame capable of acquiring all necessary orthogonal images while being able to withstand blast impacts; electrical issues complicated by discharging up to 18 flash x-ray sources simultaneously; schemes depicting how to measure the x-ray flux versus energy curves for the different flash sources; and methods to collect static data with which analysis and errors can be examined prior to completing construction of the diagnostic.

2. Discussion

2.1 Development of a Robust Structure

In order to resolve N materials, it is necessary to create N three-dimensional attenuation radiograms. For practicality, a diagnostic using three distinct flash sources with peak energies near 150–300 and 450 KeV will be constructed, in order to discern three different materials. Following the work of Moser et al. (*1*), six two-dimensional radiographs must be captured for each three-dimensional radiogram, five from around the circumference and one orthogonal. Although Moser et al. (*1*) organized their circumferential sources and imaging plate x-ray detectors on the flats of a pentagram, greater flexibility can be gained if each of the energies' source/detector pairs is mounted to a ring. The rings for each of the three energies will be stacked inside each other to create a singular symmetry point at the center, at which the object of interest is placed for examination. A schematic of this organization is shown in figure 1 (it does not show

the orthogonal view for each color), where the detectors were 355.6 × 355.6 × 50.8 mm and the tubes were between 76.2 and 150.4 mm in diameter. This integration is unique in that it allows the potential for slight flexibility of the angle at which the rings are offset from each other in one azimuth. It was also found to be beneficial to use one of the source tubes as a joining pivot point, the use of nonsymmetrical, angularly spaced tube/detector pairs within each ring (i.e., the angle between each tube/detector pair is not 72°) to eliminate overlap of detectors. Using this arrangement paired with a nominally 2-m-diameter minimum ring resulted in a fully covered cubic reconstruction space slightly greater than 160 mm in length. However, the total reconstruction space can be expanded if a low-areal density object is being imaged and an incomplete projection set is acquired.

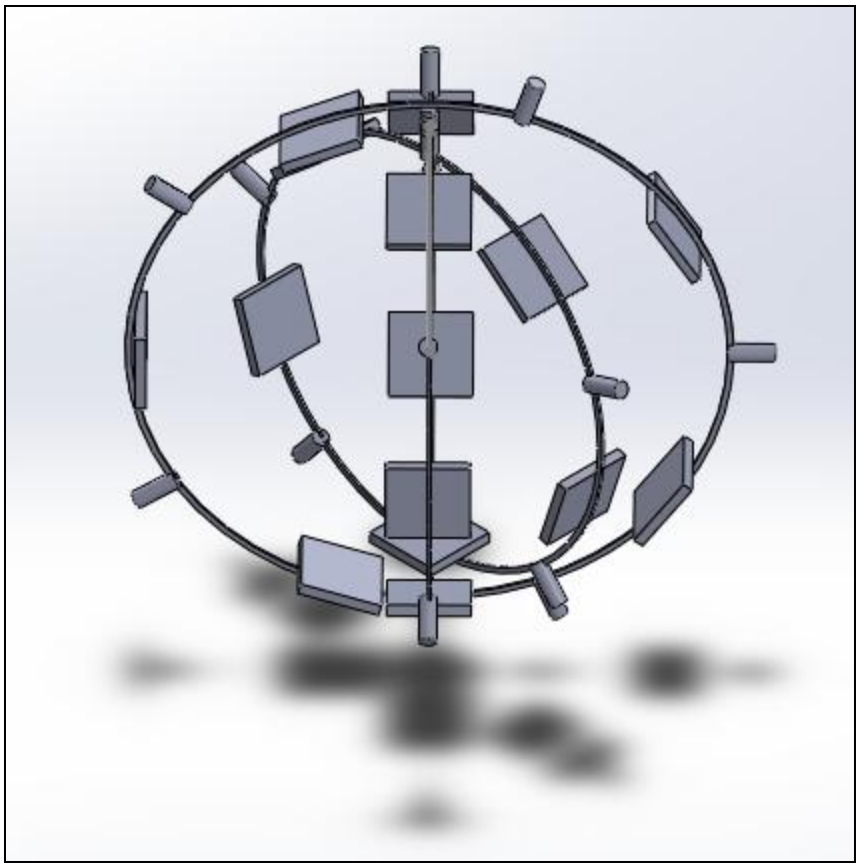

Figure 1. Computer aided drawing depiction of a potential ring structure capable of supporting the multiple x-ray sources in the geometry needed to compute three-dimensional attenuation radiographs of multiple energy sources. The drawing does not show an off-axis orthogonal x-ray source/detector pair that would be needed for each ring.

Because the diagnostic is being constructed to observe dynamic experiments that may include high-explosive driven and impact events, significant thought was put in to the robustness of the structural design. Inherently, the rings have relatively low-surface area that reduces their interaction with blast loading. This interaction can be further lowered, if needed, by applying a curved surface to the inside portion of the support member cross section as depicted in figure 2. This serves to deflect otherwise normal compression pulses and will temporally and spatially disperse the compression and rarefaction waves that transmit through the bulk of the structure, reducing the peak internal stress states. Of greater concern is the potential for portions of the ring structure to be impacted by free-flying fragments accelerated during the dynamic interactions being observed. To mitigate potential large cost and long time delays associated with reconstructing and installing a damaged ring, each ring will be designed using many pieces that will be bolted together as depicted in figure 3.

Of greater concern is the blast loading to which the detectors will be subject. Numerous effects will be possible: the loading may be asymmetric across the relatively large surface, instilling torque into the ring support structure; the loading may be such that the magnesium/ aluminum/plastic material of which the detector holders are constructed may fail; fragmentation may result in gouges of the case cover, complicating the radiographs by areas of lesser attenuation than a pristine material, etc. Many of these complications can be lessened with the implementation of two modifications to the structure pictured in figure 4. First, if the single ring is replaced with two parallel rings, the structure will be able to sustain significantly larger asymmetries in the forces exerted to/by the detector holders. Second, if the detectors are held in place using low-strength tabs, possibly made out of light metal or plastic, the tabs can shear and break free from the structure prior to transmitting a large load to the ring structure. The addition of these shear limiters to the rear of the cassette should not impede the data collection so long as the measurements are recorded prior to breaking free of their original position.

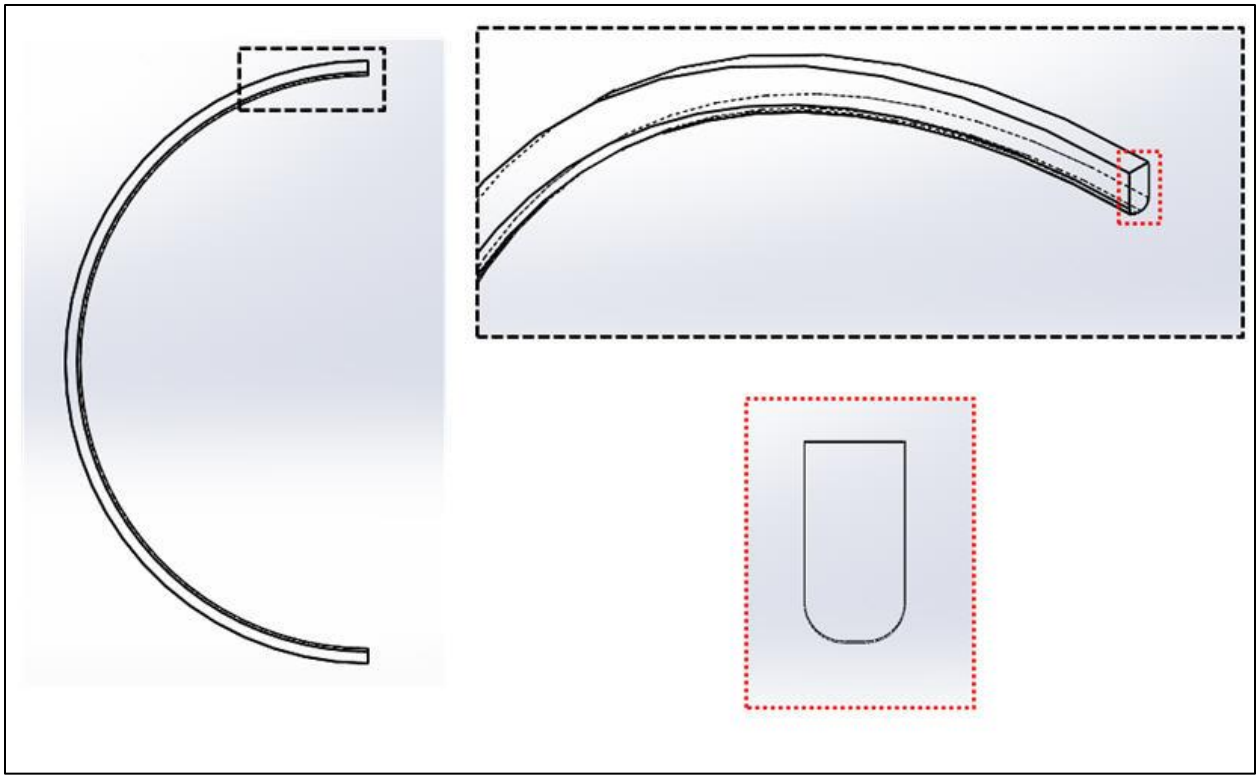

Figure 2. Cross section of ring support depicting curved internal surface to mitigate effects of impacting compression waves.

Figure 3. Schematic depicting ring support construction using multiple interchangeable pieces of steel. Two views are shown, the top depicting solid material, and the bottom depicting transparent material.

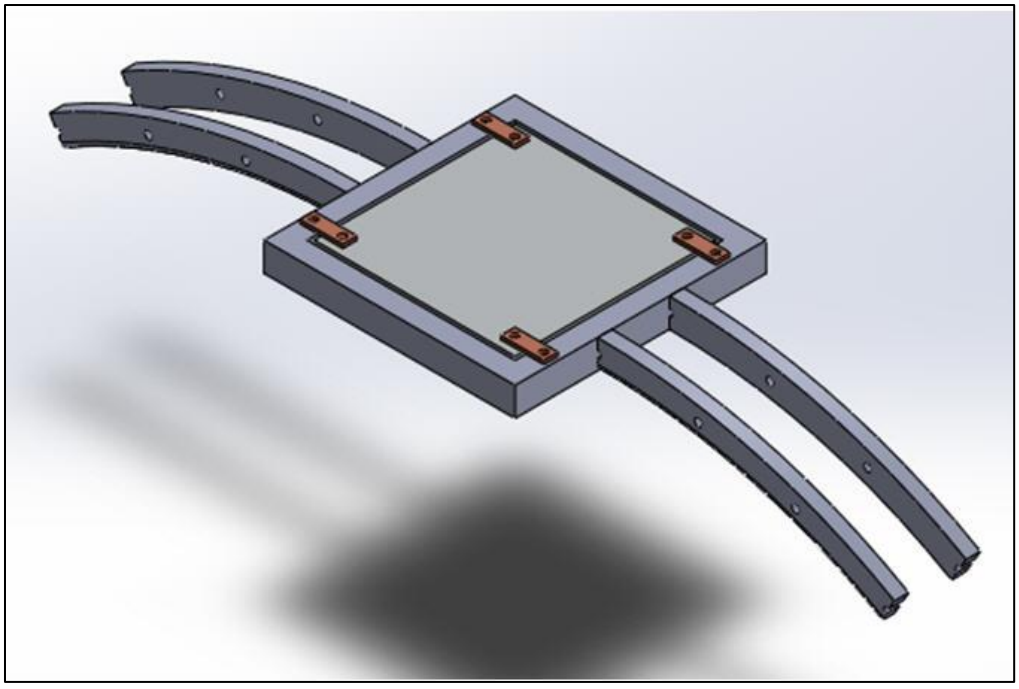

Figure 4. Schematic of the mounting provisions for the x-ray detectors (light grey) within the steel (dark grey) support structure. Of importance are the dual ring structure and the numerous shear tabs (orange).

2.2 Measurement of Flux—Energy Curve

This diagnostic's primary uniqueness relies in its ability to potentially discern materials. As mentioned in the introduction, this capability relies on the diagnostic's ability to measure geometries in three spatial dimensions, and the fact that the x-ray attenuation cross section is independent and different for each material and x-ray energy. However, because the x-ray sources produce broadband energies, the flux verses energy curve must be well-known. The manufacturers of the x-ray sources, L-3 Communications, published nominal flux verses energy curves in the operator's manual and seminar notes (p. 154 figures 4–16 in the manual) (*6*). Unfortunately, these curves are not sufficient as the actual curves depend on many factors including: the actual charge voltage of the capacitor bank; the transmission loss in the remote tube head lines; and the state of the anode and to a lesser extent the state of the cathode. To obtain more accurate curves two approaches are proposed. The first is to "reverse engineer" the curves from a series of x-radiographs taken of step wedges of known material and thickness. Figure 5 shows images of the step wedges, and table 1 lists the materials and step thicknesses. The step wedges were chosen to span a wide variety of x-ray attenuation coefficients, to populate the reverse engineered curve throughout. All wedges were constructed so that the plateaus as seen during the scattering process are nominally 25.4 × 25.4 mm, so an average signal can be measured using many pixels of a digital film detector. The second method to establish the flux verses energy curve combines peripheral interface controller PIC simulations of the diode, Monte Carlo simulations of the radiation output, and electromagnetic/circuit modeling of the

pulsed power and vacuum systems to determine the diode characteristics and x-ray output. The simulated results would then be calibrated using a detector that operates much like the step wedge method above, except that it uses an ionization chamber to get the counts of x-rays residing behind the material shielding. If this method is chosen, expertise can be found in J. Schumer's research group at the U.S. Naval Research Laboratory.

Of importance to both flux versus energy mapping methods, and during the collection of the actual experiments, is the consistency of the x-ray source (and detector). It has been considered that using step wedges in a manner similar to the first method may be necessary during the dynamic experiments to define the flux verses energy curve.

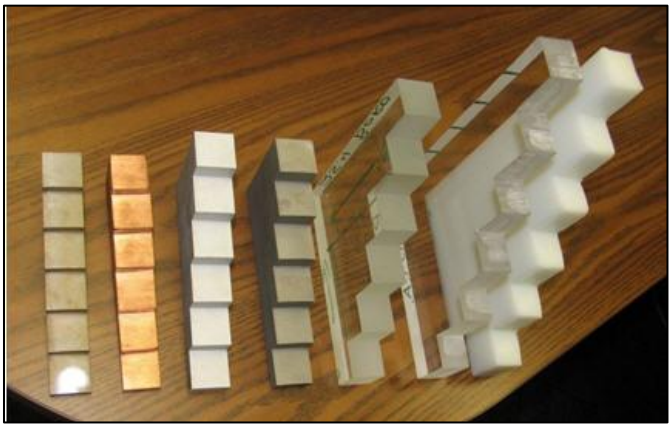

Figure 5. Photograph of the step wedges that will be employed to reverse engineer the x-ray source flux verses energy curves. All wedges were constructed so that the plateaus as seen during the scattering process are nominally 25.4 × 25.4 mm. The materials and step thicknesses are detailed in table 1 (enumerated 1 on the left [short grayish] and 7 on the right [tall white]).

Table 1. Listing of materials and thicknesses of step wedges used to calibrate the flux verse energy curves.

No.	Material	Step 1 (mm)	Step 2 (mm)	Step 3 (mm)	Step 4 (mm)	Step 5 (mm)	Step 6 (mm)
1	Steel	6.33	12.59	18.81	25.26	31.54	37.95
2	Copper	6.5	12.86	19.47	25.92	32.36	38.65
3	Al 6061	12.73	25.40	38.22	50.76	63.55	76.23
4	Ti 6Al 4V	12.96	25.59	38.22	50.93	63.59	76.27
5	Borosilicate Glass	25.44	50.86	76.24	101.66	127.06	152.44
6	Poly(methyl methacrylate)	37.04	74.65	105.55	136.52	171.83	206.18
7	Polycarbonate	36.60	70.28	103.60	137.48	171.58	204.33

2.3 Electrical Grounding, Shielding

One potential complication that may occur during discharge of the x-ray sources is the elevation of the ground potential due to an insufficient ability of an earth ground to absorb charge. This phenomenon was noted by Moser et al. (*1*) for a system in which six x-ray sources were discharged simultaneously. This could affect the potential difference between the anode/cathode pair in flash x-ray tubes, as well as interfere with supporting electronics. In anticipation of this issue, some potential grounding/shielding schemes have been considered to increase the capability of transporting charge, isolating component systems, and eliminate ground loops.

Generally, because of the relatively quick discharge times, all grounding straps will be constructed of large surface copper bands. This should promote rapid discharge of any accumulated charge by lowering path impedances. It is hypothesized that the primary charge accumulation issue relates to charge accumulation occurring in the region between the Marx generator and the x-ray tube head. This region is outlined in transparent blue for the first Marx generator/x-ray tube head pair in figure 6. This is a potential region for charge to accumulate because the error associated with the discharge timing of multiple units is greater than the time for the charge to propagate along the separation path. In an ideal situation, charge accumulated in the Marx generator 1 would propagate through the cable to the x-ray tube head 1, jump the anode/cathode gap, and then back to the Marx generator 1 (ground) via the same cable. However, if the x-ray tube heads were mounted to the metallic support structure and x-ray tube 1 discharged before x-ray tube 5, an alternate path could be established where the charge accumulated in the Marx generator 1 would propagate through the cable to the x-ray tube head 1, jump the anode/cathode gap, and then back to the Marx generator 5 (ground) via its cable. When Marx generator 5 discharges some time later, it appears as if the potential of ground has been raised, which can cause complications. To eliminate this possibility, it is suggested that the tube heads (of which the outer metallic case is the ground conductor) are insulated from the metallic ring structure. One option for placement of the insulators is pictured schematically in figure 6 (represented by the color red). In this scenario, the metallic support structure should be individually grounded.

A second precaution that could be employed is to isolate each of the three rings that will support the different energy x-ray systems independently. In this scenario, the grounding of each ring would be connected via a solid bound to the ground of each high-voltage supply individually. The transient time for any accumulated charge to propagate back through the bond to "communicate" with any other system would be longer than the temporal triggering error for the discharge of all systems, and thus would create three isolated systems.

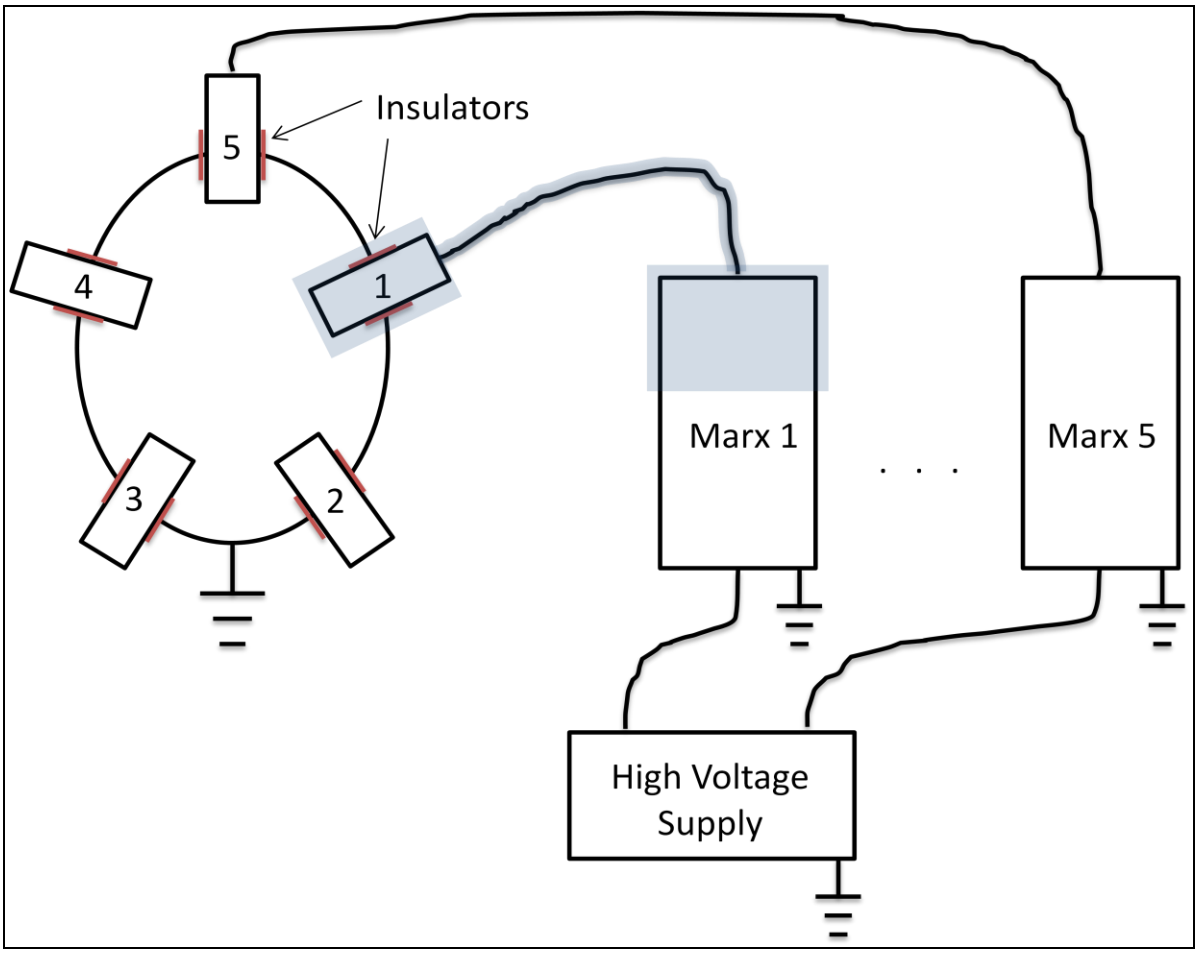

Figure 6. Schematic of system components and electrical paths.

2.4 Static Data

In order to assess the diagnostic capability prior to construction, a phantom target has been assembled that contains multiple materials imbedded inside a 127 × 127 × 127-mm poly (methyl methacrylate) block. This phantom will also serve well to assess the material and spatial resolution capabilities of the complete system once constructed. An image of the phantom is shown in figure 7 and the position, dimensions, and materials are listed in table 2. The phantom was designed so as to reside within the predicted space that will be fully sampled in the two-dimensional projections (i.e., it will not test resolution loss when an incomplete sampling of the voxel field is probed). More materials were inserted into the phantom (than the diagnostic will be available to discern), for the purpose of spanning a range of x-ray attenuation cross sections to test the resolution of material specificity. Most of the inserts have cylindrical or spherical shapes, and most hollow objects were back-filled with acrylic. One cavity was left unfilled to represent vacuum. Figures 8–13 show representative two-dimensional radiographs acquired with the phantom placed halfway between an x-ray source and imaging plate detector separated by two

meters. Sources of 450–300- and 150-KeV were compared. The images acquired with the 450- and 300-KeV sources display sufficient contrast and spatial resolution to accurately observe the position of the materials. This data will be useful in validating the reconstruction algorithm, but it will not be useful for calibrating functions of the computer program which attempt to correct for the undesired Compton scattered photons that will inevitably corrupt the images. The images acquired with the 150-KeV source show significantly less contrast. An attempt will be made to create a three-dimensional reconstruction attenuation radiograph. However, insufficient contrast may be prohibitive. This data gives the users an idea of the upper bound on material areal density through which sufficient transmission is attainable in the proposed geometry and at the lowest energies.

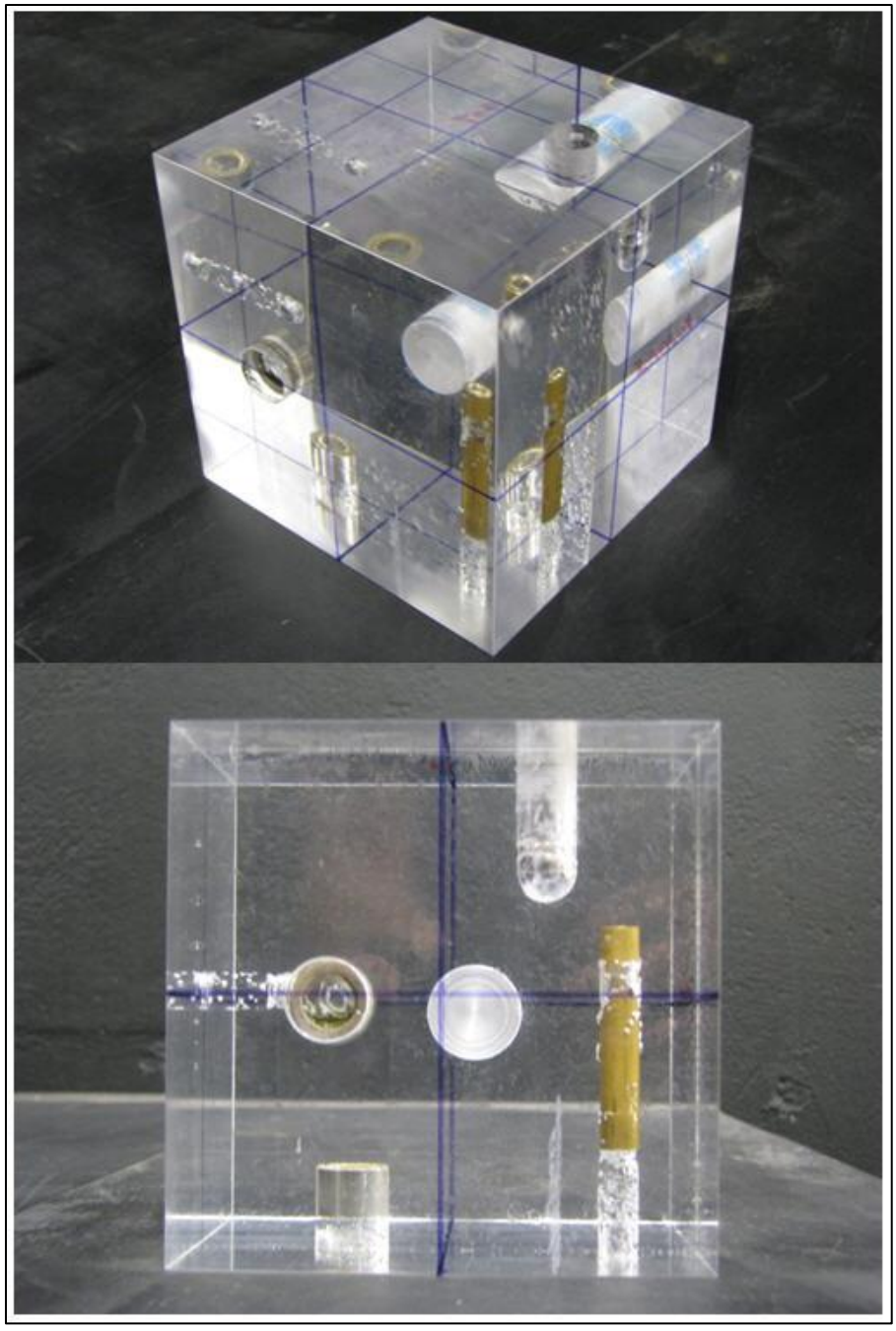

Figure 7. Photograph of the phantom target constructed for use with static testing.

Table 2. Measurements of the objects inserted into the phantom test target.

Object	Material	Length (mm)	Width (mm)	Height (mm)	X (mm)	Y (mm)	Z (mm)
Pin, solid	Aluminum	26.42	25.4	NA	57.15	69.85	26.42
Ball bearing	Steel	9.525	9.525	9.525	63.5	63.5	27.79
Ball bearing	Steel	16	16	16	38.1	88.9	—
Drill bushing, hollow (12.7-mm hole)	Steel	12.7	19.1	NA	87.02	59.11	22.23
Drill bushing, hollow (12.7-mm hole)	Steel	12.7	19.1	NA	50.8	63.246	—
Tube, hollow	Brass	52.39	9.525	NA	38.1	20.32	63.5

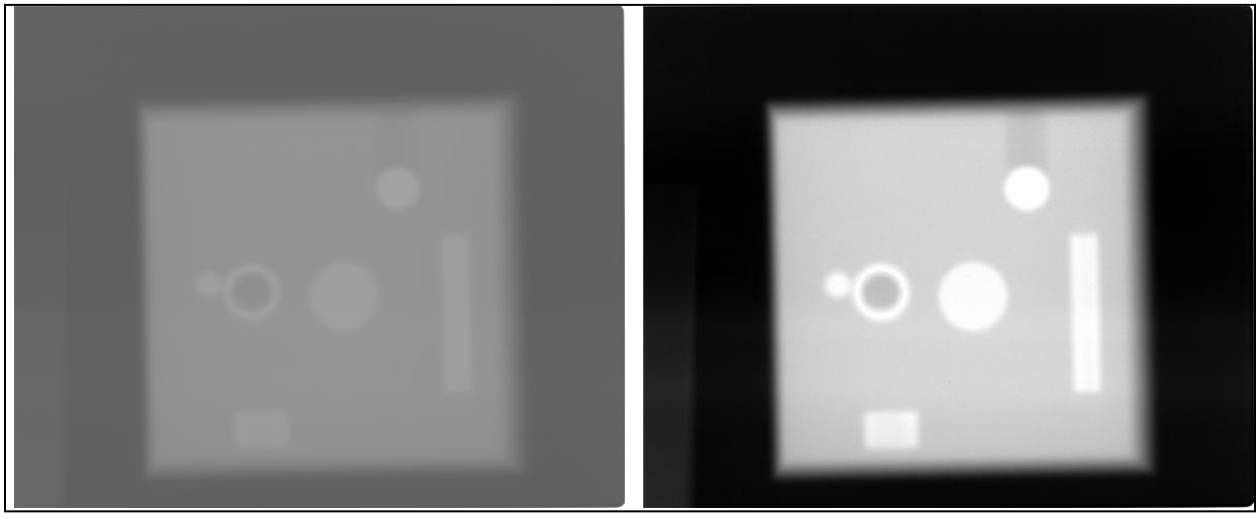

Figure 8. Representative image of the phantom target using a 450-KeV source. The image was taken at normal incidence. The left image shows the raw data file and the right image shows a contrast adjusted file.

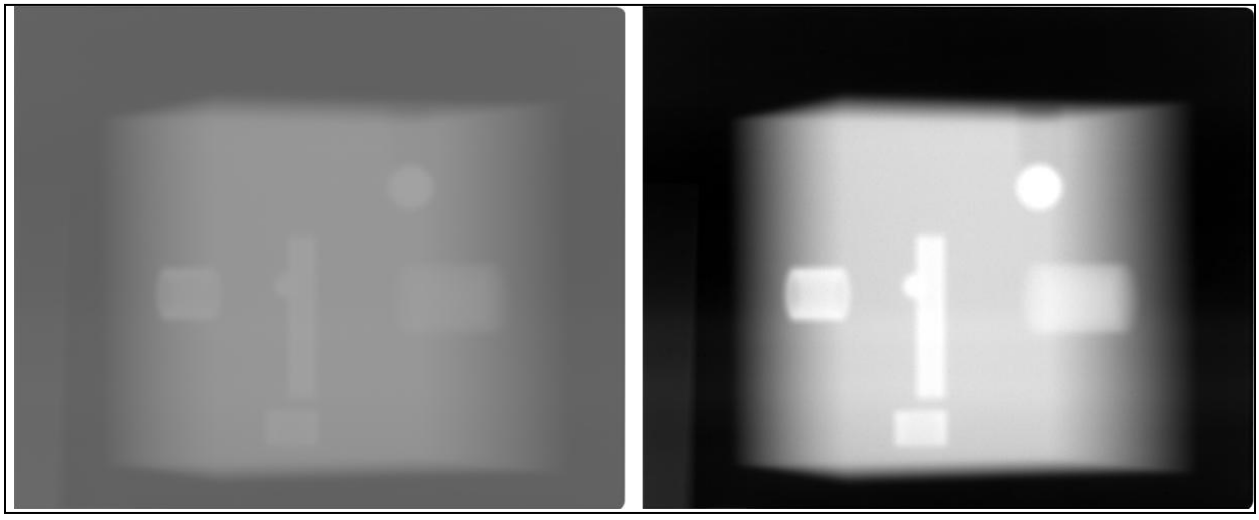

Figure 9. Representative image of the phantom target using a 450-KeV source. The image was taken 70° off of normal incidence. The left image shows the raw data file and the right image shows a contrast adjusted file.

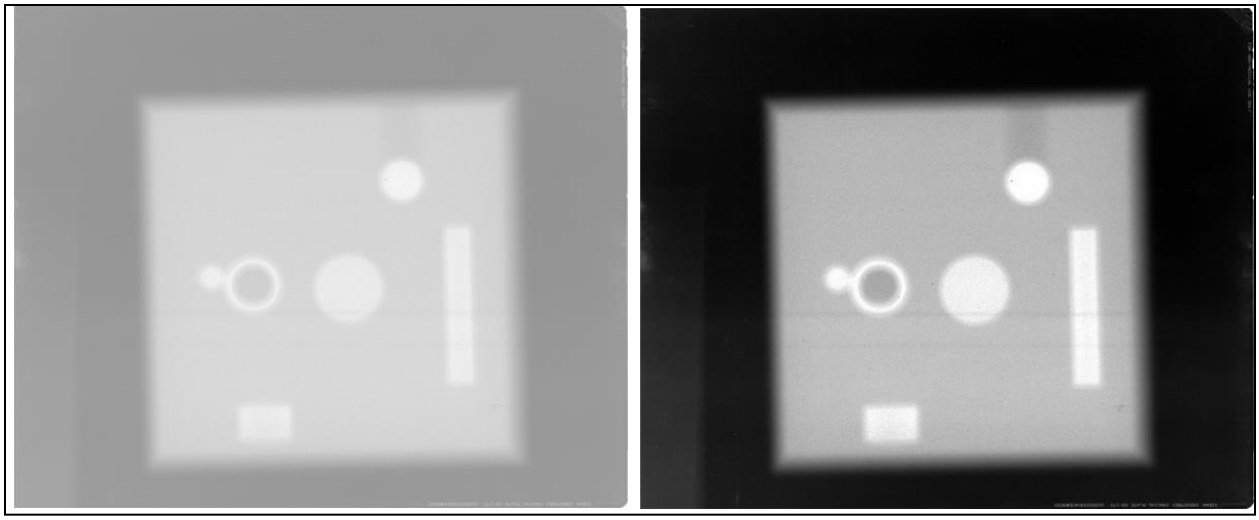

Figure 10. Representative image of the phantom target using a 300-KeV source. The image was taken at normal incidence. The left image shows the raw data file and the right image shows a contrast adjusted file.

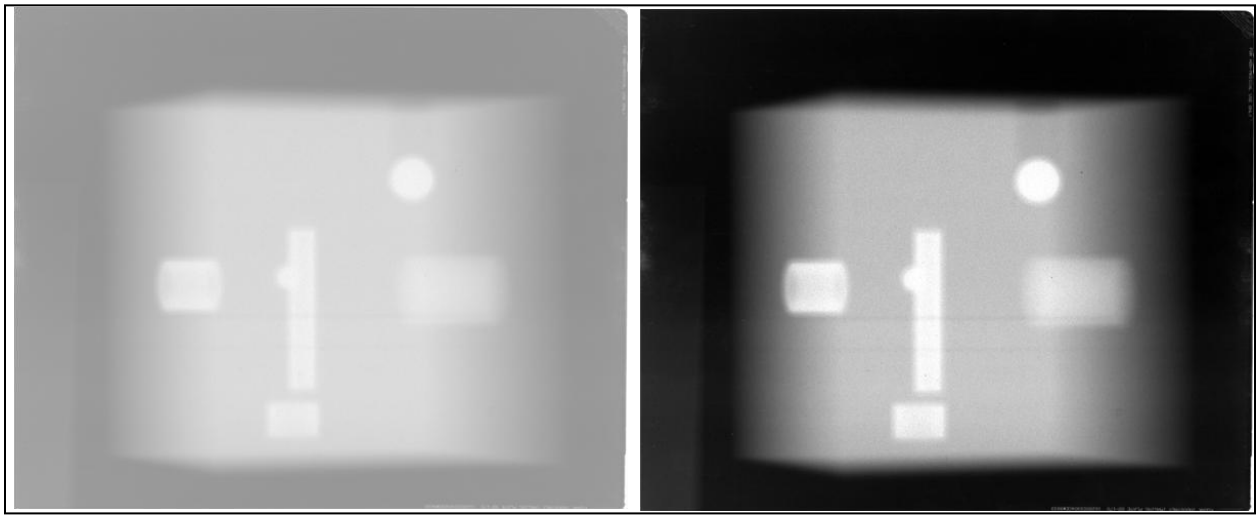

Figure 11. Representative image of the phantom target using a 300-KeV source. The image was taken 70° off of normal incidence. The left image shows the raw data file and the right image shows a contrast adjusted file.

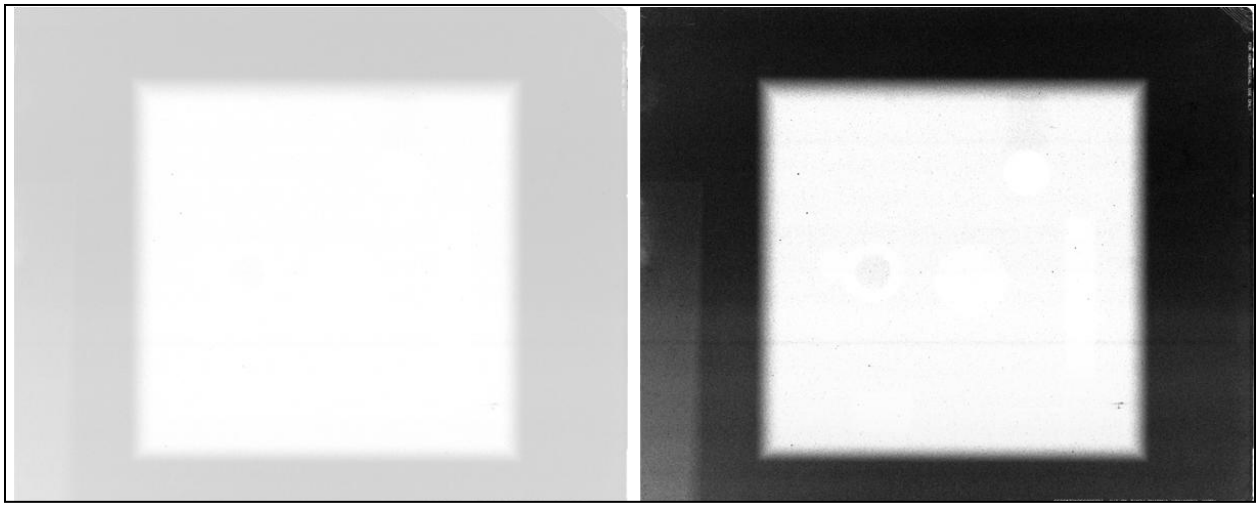

Figure 12. Representative image of the phantom target using a 150-KeV source. The image was taken at normal incidence. The left image shows the raw data file and the right image shows a contrast adjusted file.

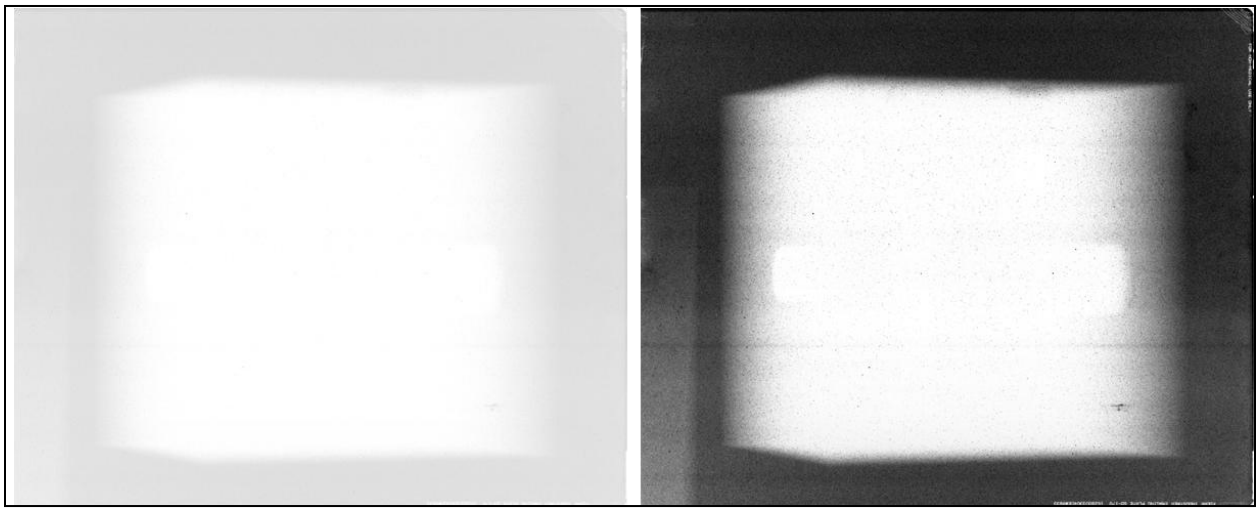

Figure 13. Representative image of the phantom target using a 150-KeV source. The image was taken 70° off of normal incidence. The left image shows the raw data file and the right image shows a contrast adjusted file.

3. Conclusions and Summary

This report discusses development of a flash x-ray computed tomography diagnostic that has the potential to differentiate between materials. This capability would significantly increase understanding of armor and materials research in that it shows promise to characterize material flow, failure, and specificity in three spatial dimensions of dynamic events. This report addresses some issues regarding test sampling, calibration and error assessment, robustness of the system to blast loading and dynamic experiments, and potential schemes to minimize undesired

electronic effects. The diagnostic would use three photon colors by using three separate x-ray energies (150, 300, and 450 KeV), simultaneously, to measure/compute three three-dimensional spatial attenuation radiographs. Because materials have an energy and wavelength specific x-ray absorption cross section, one could ratio the three-dimensional attenuation radiographs to resolve as many materials as colors of photons used (as long as only the same number of materials existed in the target, i.e., two materials and two colors). This method solves many of the experimental issues related to the Compton nature of x-ray photons and the difficulty of trying to get individual colors of photons along the same axis by applying the x-ray sources at multiple different angles and then computing the three-dimensional representation.

4. References

1. Moser, S.; Nau, S.; Manfred, S.; Klaus, T. In Situ Flash X-Ray High-Speed Computed Tomography for the Quantitative Analysis of Highly Dynamic Processes. *Meas. Sci. Technol*. **2014,** *25* 025009.

2. Schlomka, J. P.; Roessl, E.; Dorscheid, R.; Dill, S.; Martens, G.; Istel, T.; Baumer, C.; Herrmann, C.; Steadman, R; Zeitler, G.; Livne, A.; Proksa, R. Experimental Feasibility of Multi-Energy Photon-Counting K-Edge Imaging In Pre-Clinical Computed Tomography. *Phys. Med. Biol*. **2008,** *53* 4031–4047.

3. Mishra, D.; Muralidhar, K.; Munshi, P. A Robust MART Algorithm for Tomographic Applications Num. Heat. Transfer, Part B: Fundamentals: An Int. *J. Computation and Methodology* **1999,** *35* (4) 485–506.

4. Mishra, D.; Longtin, J. P.; Singh, R. P.; Prasad, V. Performance Evaluation of Iterative Tomography Algorithms for Incomplete Projection Data. *Appl. Optics* **2004,** *43* (7) 1522.

5. Hubbell, J .H.; Seltzer, S. M. Tables of X-Ray Mass Attenuation Coefficients and Mass Energy-Absorption Coefficients from 1 keV to 20 MeV for Elements Z = 1 to 92 and 48 Additional Substances of Dosimetric Interest" NISTIR5632 (1989). http://www.nist.gov/pml/data/xraycoef/ (accessed 5/27/14).

6. Drury, D.; Childers, K.; Pomeroy, S.; Lau, D.; Link, N.; Laurence, P.; Creely, B.; Kolkana, R.; Sousa, D. Flash X-Ray Seminar L-3 Pulse Sciences, San Leandro, CA.

1 (PDF) DEFENSE TECHNICAL INFORMATION CTR DTIC OCA

2 (PDF) DIRECTOR US ARMY RESEARCH LAB RDRL CIO LL IMAL HRA MAIL & RECORDS MGMT

1 (PDF) GOVT PRINTG OFC A MALHOTRA

1 (PDF) SOUTHWEST RSCH INST C ANDERSON

36 (PDF) DIR USARL
RDRL WML H
L MAGNESS
B SCHUSTER
T EHLERS
RDRL WMM B
B LOVE
RDRL WMP B
C HOPPEL
S SATAPATHY
RDRL WMP D
S ALLEYNE
A BARD
R BORYS
R DONEY
M KEELE
D KLEPONIS
H MEYER
F MURPHY
J PERRELLA
M POTTER
J RUNYEON
G SCHAFER
S SCHRAML
B SCOTT
R STRICKLAND
K STOFFEL
J STURGILL
G VUNNI
B VONK
M ZELLNER
V WAGONER
J M ZAJIECK
RDRL WMP E
S BARTUS
M BURKINS
B CHAMISH
D GALLARDY
D HACKBARTH
J HOUSKAMP
T JONES
P SWOBODA